Developmental Role and Auxin Responsiveness of Class III Homeodomain Leucine Zipper Gene Family Members in Rice[1][C][W][OA]

Jun-Ichi Itoh, Ken-Ichiro Hibara, Yutaka Sato, and Yasuo Nagato*

Graduate School of Agricultural and Life Sciences, University of Tokyo, Tokyo 113–8657, Japan (J.-I.I., K.-I.H., Y.N.); and Department of Biological Mechanisms and Functions, Graduate School of Bioagricultural Sciences, Nagoya University, Nagoya 464–8601, Japan (Y.S.)

Members of the Class III homeodomain leucine zipper (Class III HD-Zip) gene family are central regulators of crucial aspects of plant development. To better understand the roles of five Class III HD-Zip genes in rice (*Oryza sativa*) development, we investigated their expression patterns, ectopic expression phenotypes, and auxin responsiveness. Four genes, *OSHB1* to *OSHB4*, were expressed in a localized domain of the shoot apical meristem (SAM), the adaxial cells of leaf primordia, the leaf margins, and the xylem tissue of vascular bundles. In contrast, expression of *OSHB5* was observed only in phloem tissue. Plants ectopically expressing *microRNA166*-resistant versions of the *OSHB3* gene exhibited severe defects, including the ectopic production of leaf margins, shoots, and radialized leaves. The treatment of seedlings with auxin quickly induced ectopic *OSHB3* expression in the entire region of the SAM, but not in other tissues. Furthermore, this ectopic expression of *OSHB3* was correlated with leaf initiation defects. Our findings suggest that rice Class III HD-Zip genes have conserved functions with their homologs in Arabidopsis (*Arabidopsis thaliana*), but have also acquired specific developmental roles in grasses or monocots. In addition, some Class III HD-Zip genes may regulate the leaf initiation process in the SAM in an auxin-dependent manner.

In flowering plants, elaboration of the shoot architecture depends primarily on the activity of the shoot apical meristem (SAM). The SAM of seed plants consists of two distinct histological domains: the central zone, with a low cell division rate, and the peripheral zone, where leaf primordia initiate with a high rate of cell division (Steeves and Sussex, 1989). Once a leaf primordium initiates from the peripheral zone of the SAM, it usually displays polarities along the proximal-distal and adaxial-abaxial axes. The SAM in flowering plants first initiates at a fixed position in the embryo after the embryonic pattern is established. These patterning events are universal among these plant species, and the diversity of plant architecture largely depends on spatial and temporal modifications of subsequent events.

To build a highly complex plant form, the precise spatial and temporal expression of regulatory genes is essential. Among several other regulatory genes, members of the Class III homeodomain Leu zipper (Class III HD-Zip) family are regulators of key aspects of plant development. Class III HD-Zip genes encode transcriptional regulators containing a homeodomain for DNA binding and a Leu-zipper domain for dimer formation (Sessa et al., 1998), an N-terminal putative lipid- or steroid-binding START domain (Ponting and Aravind, 1999), and a C-terminal MEKHLA domain that potentially functions as a sensory and/or protein interaction domain (Mukherjee and Bürglin, 2006; Chandler et al., 2007). In Arabidopsis (*Arabidopsis thaliana*), there are five Class III HD-Zip genes: *REVOLUTA* (*REV*)/*AMPHIVASAL VASCULAR BUNDLE1* (*AVB1*), *PHABULOSA* (*PHB*), *PHAVOLUTA* (*PHV*), *CORONA* (*CNA*)/*INCURVATA4* (*ICU4*), and *ATHB8*. Phenotypic analysis of loss-of-function mutants of these genes has revealed that the genes have overlapping, antagonistic, and distinct roles in development (Emery et al., 2003; Prigge et al., 2005). *REV*, *PHV*, and *PHB* appear to play a role in the establishment of the SAM and the adaxial identity of the lateral organs. Although single mutations in *PHB* and *PHV* result in almost normal phenotypes, the triple mutant *phb phv rev* shows a single radial cotyledon and lack of the SAM in the embryo (Emery et al., 2003; Prigge et al., 2005). Dominant gain-of-function mutants of Class III HD-Zip genes in Arabidopsis show meristem and leaf polarity defects (McConnell and Barton, 1998; McConnell et al., 2001; Zhong and Ye, 2004; Ochando et al., 2006).

[1] This work was supported in part by Grants-in-Aid for Scientific Research from the Ministry of Education, Culture, Sports, Science, and Technology of Japan (20248001 to Y.N. and 17780003 and 20061005 to J.-I.I.).

* Corresponding author; e-mail anagato@mail.ecc.u-tokyo.ac.jp.

The author responsible for distribution of materials integral to the findings presented in this article in accordance with the policy described in the Instructions for Authors (www.plantphysiol.org) is: Yasuo Nagato (anagato@mail.ecc.u-tokyo.ac.jp).

[C] Some figures in this article are displayed in color online but in black and white in print.

[W] The online version of this article contains Web-only data.

[OA] Open Access articles can be viewed online without a subscription.

www.plantphysiol.org/cgi/doi/10.1104/pp.108.118679

Consistent with their role in the SAM and the adaxial identity of the lateral organs, all three of these genes are expressed in the SAM and in the adaxial domain of the lateral organs (Zhong and Ye, 1999; McConnell et al., 2001; Otsuga et al., 2001; Emery et al., 2003; Prigge et al., 2005). In contrast, *CNA* and *ATHB8* have functions antagonistic to *REV*, because mutations in *CNA* and *ATHB8* suppress meristem defects of *rev* mutants (Prigge et al., 2005).

Class III HD-Zip genes also regulate vascular patterning and differentiation. Loss of *REV* activity causes defects in the formation of interfascicular fibers that are enhanced by mutations in *PHB* and *PHV* (Talbert et al., 1995; Zhong et al., 1997; Zhong and Ye, 1999; Emery et al., 2003; Prigge et al., 2005). Dominant gain-of-function mutants of *PHB*, *PHV*, and *REV* show radialized vascular bundles with xylem surrounding phloem (McConnell and Barton, 1998; Emery et al., 2003; Zhong and Ye, 2004).

Polarized Class III HD-Zip expression and the roles of these genes in lateral organs and vascular patterning depend on posttranscriptional regulation by microRNA*165/166* (Reinhart et al., 2002; Rhoades et al., 2002; Tang et al., 2003). Dominant gain-of-function alleles of *phb-d*, *phv-d*, *rev-d*, *avb1*, and *icu4* in Arabidopsis and *rld1* in maize (*Zea mays*) have a single nucleotide change within the *miR165/166*-recognition sequence, and the *miR165/166*-dependent cleavage of their transcripts is suppressed, resulting in the ectopic expression of their gene products (McConnell et al., 2001; Emery et al., 2003; Juarez et al., 2004; Zhong and Ye, 2004; Ochando et al., 2006).

Several genes genetically interact with Class III HD-Zip genes in Arabidopsis. *KANADI* (*KAN*) genes have an antagonistic function to Class III HD-Zip genes (Kerstetter et al., 2001; Eshed et al., 2004). *KAN* genes are generally expressed in domains complementary to those where Class III HD-Zip genes are expressed, and multiple loss-of-function mutants of *kan* genes exhibit similar polarity defects as gain-of-function mutants of Class III HD-Zip genes (Eshed et al., 2001, 2004; Kerstetter et al., 2001; Emery et al., 2003). Furthermore, in the *kan1 kan2 kan4* background, *PHB* is expressed throughout leaf primordia (Eshed et al., 2004). Loss of the activity of the *DORNRÖSCHEN* (*DRN*) and *DRN-LIKE* (*DRNL*) genes results in embryonic defects similar to those caused by the loss of Class III HD-Zip activity and the DRN and DRNL proteins physically interact with Class III HD-Zip (Chandler et al., 2007).

The close association of *KAN* and *DRN* with auxin and/or auxin flow has been suggested. The triple mutant *kan1 kan2 kan4* shows aberrant distribution of the auxin efflux carrier protein PIN1, resulting in ectopic auxin maxima and ectopic organ formation in the embryo (Izhaki and Bowman, 2007). Similarly, in the *drn-1* mutant background, the abnormal expression of the auxin reporter genes *DR5::GFP* and *PIN1::PIN1-GFP* are observed in the embryo (Chandler et al., 2007). Although a close association between the Class III HD-Zip-mediated genetic pathway and auxin and/or auxin flow has been suggested (Baima et al., 1995; Zhong and Ye, 2001; Bowman and Floyd, 2008), it is unknown how Class III HD-Zip genes interact with auxin.

Class III HD-Zip genes are good genetic markers for understanding morphological and developmental innovations achieved during the evolutionary history of land plants, because the Class III HD-Zip gene family has been found in all land plant lineages (Floyd and Bowman, 2004; Floyd et al., 2006). In addition, expression analyses have suggested that Class III HD-Zip genes have an important developmental role in all land plants (Floyd et al., 2006; Prigge and Clark, 2006). However, the understanding of the diversity and conservation of the developmental roles of these genes is limited. In addition, there are unanswered questions concerning the roles of Class III HD-Zip genes in the leaf initiation process and their relationship to auxin.

In this study, we investigated the expression patterns, ectopic expression phenotypes, and auxin responsiveness of rice (*Oryza sativa*) Class III HD-Zip genes for understanding their developmental roles in rice.

RESULTS

Gene Structure and Phylogenetic Relationship of Rice Class III HD-Zip Genes

The rice genome contains five Class III HD-Zip genes: *OSHB1* to *OSHB5* (Zhong and Ye, 2004). Recently, a genome-wide survey of HD-Zip genes in rice also detected five Class III HD-Zip genes: *Oshox10*, *Oshox9*, *Oshox33*, *Oshox32* and *Oshox29*, corresponding to *OSHB1* to *OSHB5*, respectively (Agalou et al., 2008). We searched for full-length cDNAs of each of the five *OSHB* genes in a gene database, and found four full-length cDNAs corresponding to *OSHB1* to *OSHB4*. Because no full-length cDNA for *OSHB5* was found in the database, we isolated the full-length cDNA directly and determined its sequence. The coding region of the *OSHB5* cDNA comprises 2,607 nucleotides, the longest of the five *OSHB* genes. Comparison of the cDNA and genomic sequences revealed that there are 17 internal introns in *OSHB1* to *OSHB4*, with well-conserved splice sites, although *OSHB3* and *OSHB4* have longer first introns than *OSHB1* and *OSHB2* (Fig. 1A). In contrast to the well-conserved exon-intron organization in *OSHB1* to *OSHB4*, *OSHB5* has only 15 introns, lacking two introns corresponding to the first and second introns of the other *OSHB* genes.

The *miR166*-binding sequence is completely conserved in the five *OSHB* cDNAs (Supplemental Fig. S1B), but it is interrupted by the fourth intron in *OSHB1* to *OSHB4* and by the second intron in *OSHB5* (Fig. 1A).

All of the five OSHB proteins contain highly conserved homeodomain, Leu-zipper domains and START domains (Fig. 1A; Supplemental Fig. S1A). Phylogenetic analyses of the Class III HD-Zip genes in several angiosperm species have revealed that the genes are resolved into two monophyletic groups referred to as the REV/RBV clade and the CNA/C8 clade, although

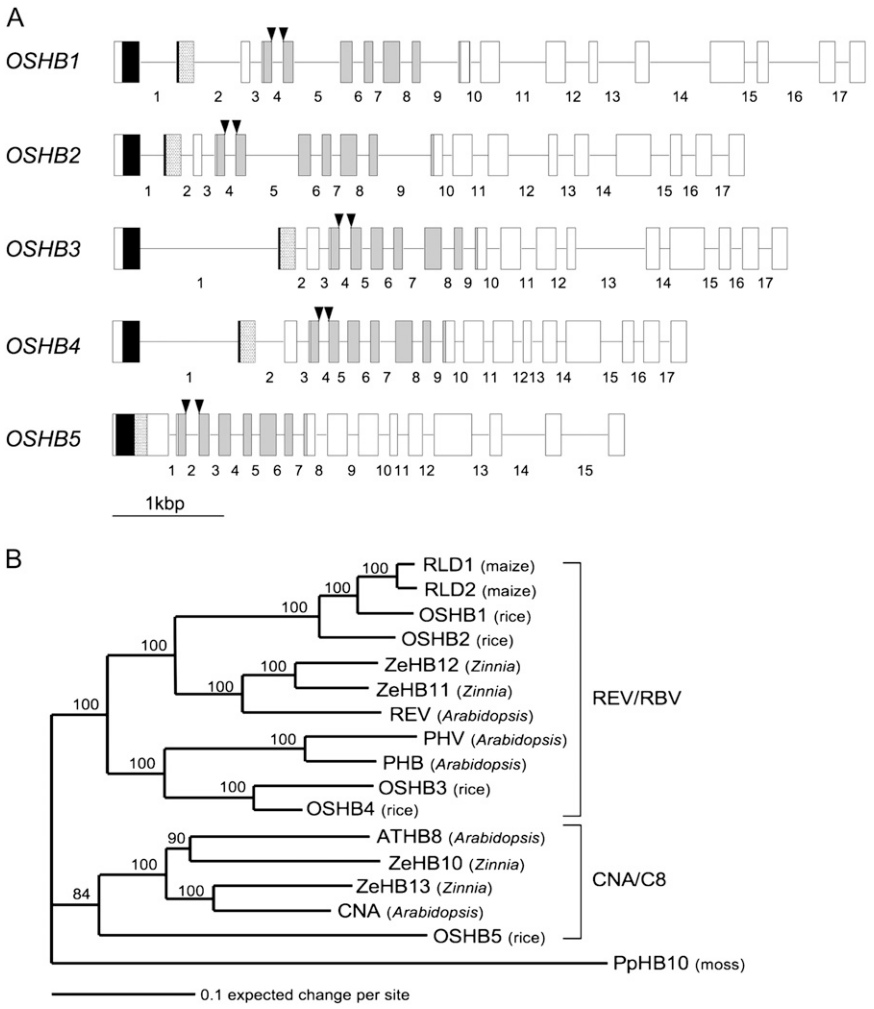

Figure 1. Structural and phylogenetic relationship among Class III HD-Zip genes in rice. A, Exon-intron structure of five *OSHB* genes. Exons are presented by boxes, and introns by bars. Introns within the cording region are numbered. Exons in black, dotted, and light gray boxes indicate the position of the homeodomain, Leu zipper, and START domains, respectively. Arrowheads indicate the *miR166*-binding site. B, Phylogenetic tree of HD-ZIP III proteins in several angiosperms rooted by PpHB10. Numbers above the branches indicate bootstrap values calculated from 1,000 replicates.

both the clades originally include gymnosperm sequences (Floyd et al., 2006; Prigge and Clark, 2006; Fig. 1B). *OSHB1* to *OSHB4* belong to the REV/RBV clade, and *OSHB5* belongs to the CNA/C8 clade. *OSHB1* and *OSHB2* are orthologs of *REV* in Arabidopsis, together with its sister genes in *Zinnia*, *ZeHB11*, and *ZeHB12*. Two maize (*Zea mays*) genes, *RLD1* and *RLD2*, are sisters of *OSHB1*. *OSHB3* and *OSHB4* are orthologous to both *PHB* and *PHV* in Arabidopsis. Two Arabidopsis genes, *ATHB8* and *CNA*, are orthologous to *ZeHB10* and *ZeHB13* of *Zinnia*, respectively. However, *OSHB5* is a single sister gene to both Arabidopsis and *Zinnia* genes in the CNA/C8 clade. This phylogenetic relationship is supported by previous reports (Zhong and Ye, 2004; Floyd et al., 2006; Prigge and Clark, 2006). These results suggest that the five *OSHB* genes in rice retain conserved molecular functions with other Class III HD-Zip genes of angiosperms.

Overall Expression Patterns of the *OSHB* Genes

We first investigated the expression levels of the *OSHB* genes in various organs and tissues using real-time reverse transcription (RT)-PCR. All of the five *OSHB* genes were expressed in all of the tissues; shoot and inflorescence apices, immature leaves, panicles, flowers, embryos, and roots, although their expression levels varied widely by gene and tissue (Supplemental Fig. S2). The transcript levels of *OSHB1* and *OSHB2* were low in developing embryo and root, and moderate in other tissues. The expression of *OSHB3* and *OSHB4* was strong in the inflorescence tissues and moderate in other tissues. *OSHB5* showed a different expression profile from the other *OSHB* genes; its mRNA accumulated to low levels in young leaves, developing embryo and flowers, but to moderate levels in the inflorescence tissues and root. Thus, the *OSHB* genes may function in all the organs and tissues that we examined, but display some level of tissue-specific expression.

Expression Patterns of *OSHB* Genes during Embryogenesis

To better understand the spatiotemporal expression patterns of the *OSHB* genes, we examined their ex-

pression by in situ hybridization. First, we investigated *OSHB* expression in the embryo. A review of rice embryogenesis and the developmental stages of the embryo was published by Itoh et al. (2005). To summarize, for 3 d after pollination (DAP), the rice embryo remains globular, with no morphological differentiation visible. At 4 DAP, the embryonic SAM and coleoptile primordium are formed in the apical and ventral positions of the embryo, and the radicle primordium is formed in the basal region. At 5 DAP, the embryonic SAM produces the first foliage leaf, and by 8 DAP, the morphological differentiation of the rice embryo is almost complete.

Expression of *OSHB1*, *OSHB3*, and *OSHB4* was detected in the center and ventral domains of the embryo at the late globular stage (3 DAP; Fig. 2, A, C, and D). The central expression domain corresponds to the place where the vasculature will differentiate, and the ventral domain corresponds to the site where the SAM will later initiate. The central expression of *OSHB3* was observed as early as the middle globular stage (2 DAP; Fig. 2C, inset). *OSHB2* expression was first detected in a small region of the ventral surface corresponding to the presumptive SAM of the late globular embryo (Fig. 2B). At 4 DAP, when the coleoptile primordium and the SAM were visible, *OSHB1*, *OSHB3*, and *OSHB4* were expressed in the SAM, the adaxial domain of the coleoptile, and the provascular tissue (Fig. 2, F, H, and I). *OSHB2* was weakly expressed in the SAM and adaxial cells of the coleoptile (Fig. 2G). At 5 DAP, when the SAM produced the first leaf primordium, the expression of *OSHB1* to *OSHB4* was detected in similar domains as at 4 DAP (Fig. 2, K–N). Their expression persisted in part of the SAM, the vascular bundles, the adaxial cells of the coleoptile, and the first leaf primordium, and expression of *OSHB2* was also detected over the entire surface (L1) of the SAM (Fig. 2L). In contrast, *OSHB5* transcripts were first detectable at 6 to 7 DAP only in the vascular bundle of the basal portion of the radicle (Fig. 2, E, J, and O). *OSHB5* expression in the radicle was observed in two separate cell files of the vascular bundle. This expression pattern in the vascular bundle was quite different from that of the other *OSHB* genes, whose transcripts were detected in the center (Fig. 2N). This indicates that *OSHB5* is expressed in a specific cell type of the vascular bundle.

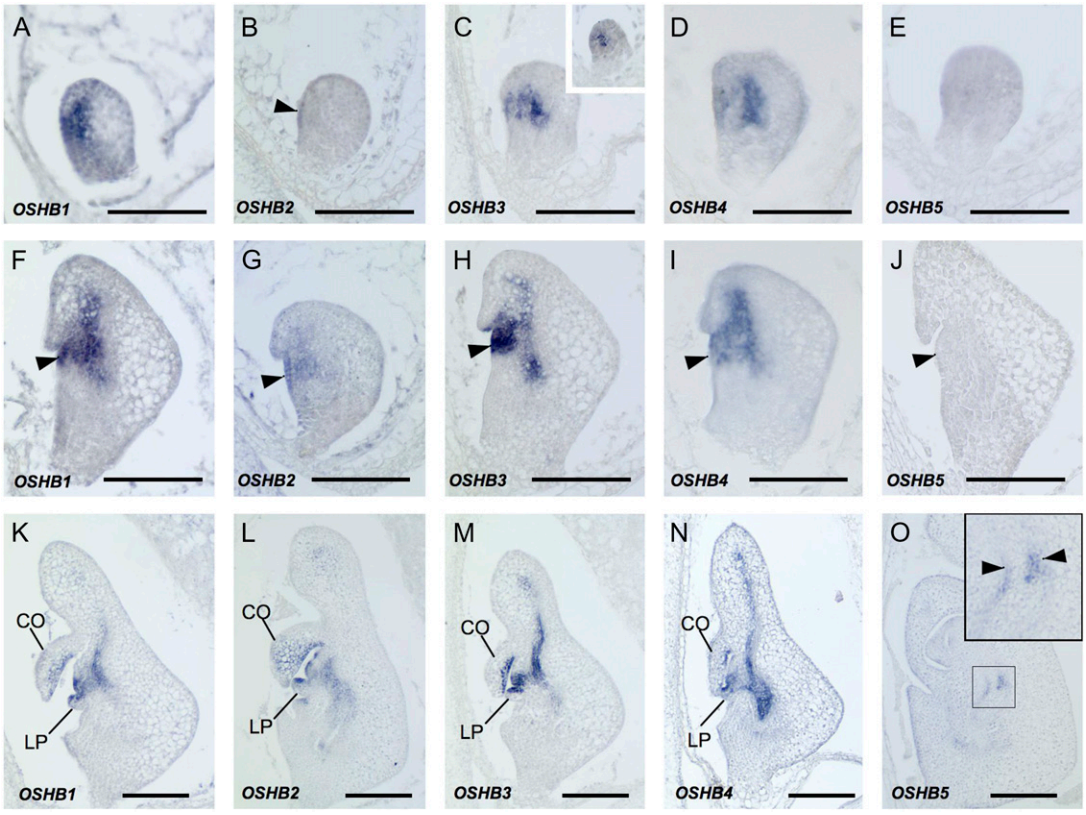

Figure 2. In situ localization of *OSHB* transcripts in embryo. A to O, Longitudinal sections of wild-type embryos at 3 DAP (A–E), 4 DAP (F–J), 5 DAP (K–N), and 7 DAP (O). A, F, and K, *OSHB1* expression. B, G, and L, *OSHB2* expression. C, H, and M, *OSHB3* expression. Arrowhead in C indicates *OSHB2* expression in the ventral surface of the embryo. The inset in C shows *OSHB3* expression at 2 DAP. D, I, and N, *OSHB4* expression. E, J, and O, *OSHB5* expression. The inset in O shows a higher magnification view of the signal in the box. Signals are observed in two cell files (arrowheads) in the vascular tissue. Arrows in F to J indicate SAMs. CO, Coleoptile; LP, leaf primordium. Scale bars = 100 μm.

Expression Patterns of the *OSHB* Genes in Vegetative Development

Next, we observed *OSHB* expression in the vegetative shoot apex. In seedlings at 2 weeks after germination, the expression of *OSHB1* to *OSHB4* was detected in the SAM, adaxial cells of the leaf primordia, and vascular tissue (Fig. 3, A–D and F–I), although slight differences were observed between the genes, as described below. In contrast, *OSHB5* was weakly expressed in vascular bundles and in the tip of the P1 leaf primordium, but not in the SAM or adaxial cells of the leaf primordia (Fig. 3, E and J).

The expression patterns of *OSHB1* to *OSHB4* in the SAM appeared to change during the plastochron. In most of the shoot apices sampled, signals were limited to the central domain of the SAM and were not detected in the P0 leaf primordium (Fig. 3, A–D). Detailed examination of *OSHB1* and *OSHB3*, however, revealed that once the P1 leaf primordium became visible as a protrusion, *OSHB1* and *OSHB3* expression rapidly extended from the central domain of the SAM toward the leaf initiation site (Fig. 3, K and M). This enlarged expression domain in the SAM was maintained until the middle P1 stage (Fig. 3, L and N), and then the signals became confined again to the central domain of the SAM (Fig. 3, A and C). Thus, the expression domain of *OSHB1* and *OSHB3* in the SAM changes drastically during the plastochron.

The expression patterns of *OSHB1* to *OSHB4* in leaf primordia were similar (Fig. 3, A–D and F–I). In the P1 primordium, the expression of *OSHB1* and *OSHB3* was restricted to the adaxial cells and a few cells in the leaf margins (Fig. 3, O and P). In the P3 leaf primordium, the expression of *OSHB1* and *OSHB2* extended to bundle sheath extension cells (Fig. 3, F and G), whereas *OSHB3* and *OSHB4* expression was limited to the adaxial surface and the vascular bundle (Fig. 3, H and I). The expression of *OSHB1* and *OSHB3* in the leaf margins was retained at this stage (Fig. 4, Q and R). In the P4 leaf primordium, strong *OSHB3* expression was evident in the adaxial sclerenchymatous cells (Fig. 3S) and in the adaxial cells of the ligule primordium (Fig. 3T).

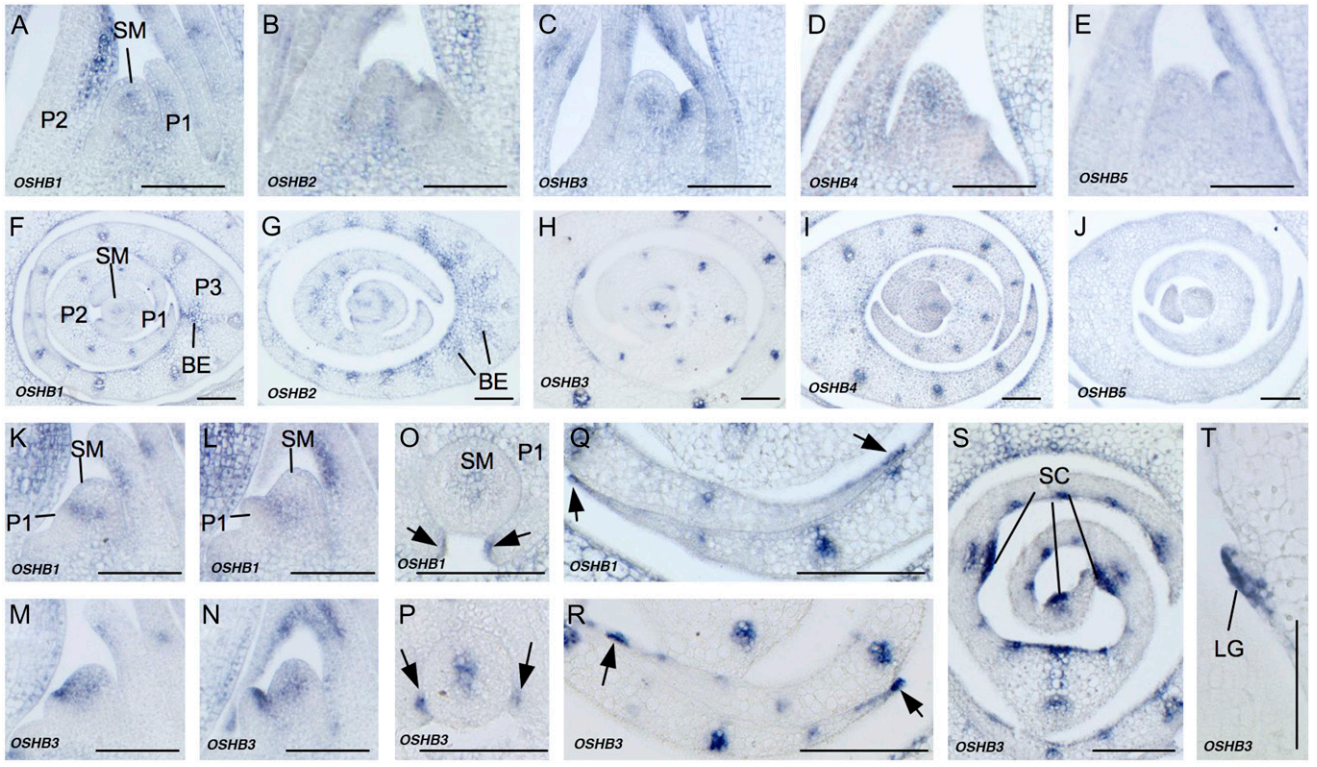

Figure 3. In situ localization of *OSHB* transcripts in the vegetative shoot apex. A to E, K to N, and T, Longitudinal sections of 2-week-old wild-type shoot apices. F to J and O to S, Cross sections of 2-week-old wild-type shoot apices. A and F, *OSHB1* expression. B and G, *OSHB2* expression. C and H, *OSHB3* expression. D and I, *OSHB4* expression. E and J, *OSHB5* expression. K, *OSHB1* expression in shoot apex when the P1 primordium is just protruded. L, *OSHB1* expression in the shoot apex when the P1 primordium is developing. M, *OSHB3* expression in the shoot apex when the P1 primordium is just protruded. N, *OSHB3* expression in the shoot apex when the P1 primordium is developing. O, *OSHB1* expression in P1 leaf margins (arrows). P, *OSHB3* expression in P1 leaf margins (arrows). Q, *OSHB1* expression in P3 leaf margins (arrows). R, *OSHB3* expression in P3 leaf margins (arrows). S, *OSHB3* expression in the P3 leaf blade, shown in adaxial sclerenchymatous cells (SC). T, *OSHB3* expression in the ligule primordium (LG) of the P3 leaf. SM, SAM; P1, P1 leaf primordium; P2, P2 leaf primordium; P3, P3 leaf primordium; BE, bundle sheath extension. Scale bars = 100 μm.

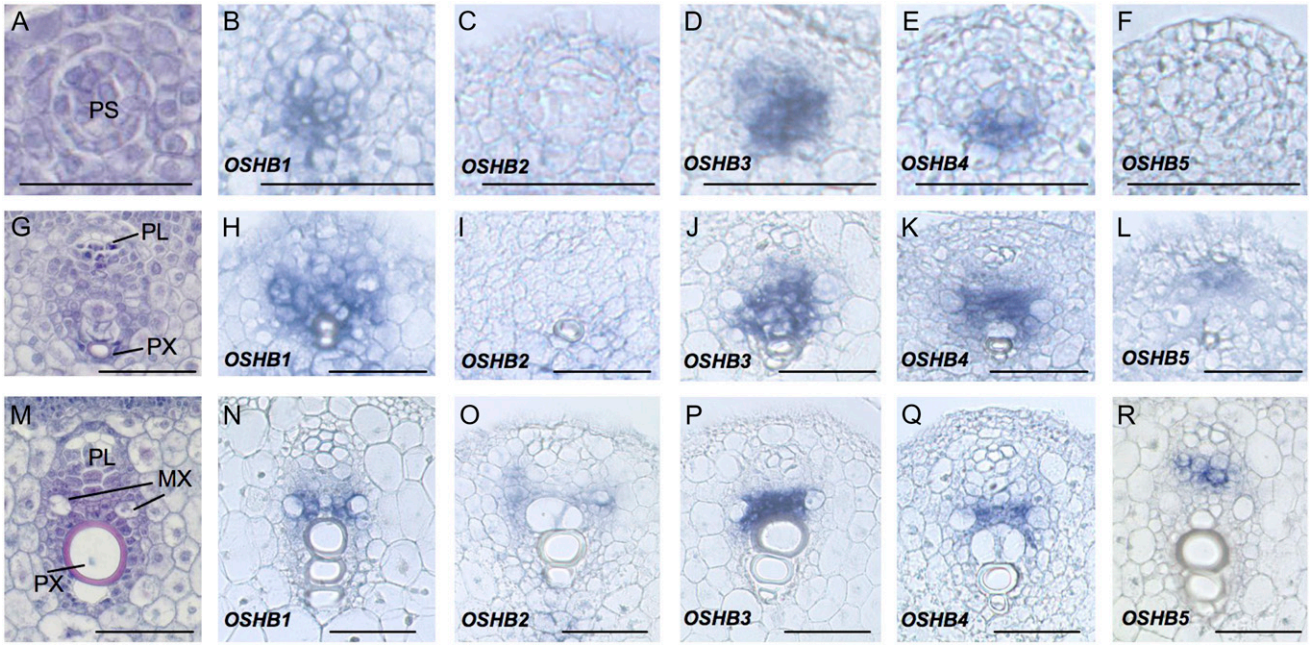

Figure 4. In situ localization of *OSHB* transcripts during vascular development. A to F, Early stage of vascular development when procambial strands are evident. G to L, Middle stage of vascular development when the protophloem and protoxylem are visible. M to R, Late stage of vascular development when the metaxylem is evident. A, G, and M, Wild-type vascular bundle stained with hematoxyline, safranin, and Fast-Green FCF. B, H, and N, *OSHB1* expression. C, I, and O, *OSHB2* expression. D, J, and P, *OSHB3* expression. E, K, and Q, *OSHB4* expression. F, L, and R, *OSHB5* expression. PS, Procambial strand; PL, protophloem; PX, protoxylem; MX, metaxylem. Scale bars = 100 μm.

To better understand how the rice *OSHB* genes are associated with vascular development, we examined the expression dynamics of these genes during vascular development (Fig. 4, A, G, and M). Signals of *OSHB1*, *OSHB3*, and *OSHB4* were first observed in a group of procambium cells of late P1 to early P2 primordia (Fig. 4, B, D, and E). As cellular differentiation progressed, mRNAs of these *OSHB* genes accumulated in the region where the xylem would develop (Fig. 4, H, J, and K), with the expression domain of *OSHB1* larger than those of *OSHB3* and *OSHB4* (Fig. 4, H, J, and K). At the late stage of vascular development, when cellular differentiation was being completed, expression of these genes continued in the cells between the metaxylem elements (Fig. 4, N, P, and Q). *OSHB2* mRNA accumulated in a domain of the vascular tissue similar to the area where the *OSHB1*, *OSHB3*, and *OSHB4* mRNAs accumulated at the late stage (Fig. 4O), but the signal was not detected at the early stage (Fig. 4, C and I). In contrast, the *OSHB5* expression pattern was distinct from that of the other genes. No *OSHB5* signal was observed in the early stage of vascular development (Fig. 4F), but signal was detected in the phloem tissue as cellular differentiation progressed (Fig. 4, L and R). This *OSHB5* expression pattern corresponded to that in the embryo (Fig. 2O). Thus, the function of *OSHB5* in vascular development may be different from that of the other *OSHB* genes. The expression profile of *OSHB* genes in leaf vasculature suggests a possibility that *OSHB* genes share overlapping but distinct functions in vascular development.

In the reproductive phase, the expression pattern of each *OSHB* gene was similar to that in the vegetative phase. However, the down-regulation of *OSHB1*, *OSHB3*, and *OSHB4* in the L1 and L2 layers was not observed in the inflorescence meristem (Supplemental Fig. S3, A, C, and D). In addition, *OSHB2* expression was not observed in the center of the inflorescence or the floral meristems (Supplemental Fig. S3, C and G), and weak *OSHB5* expression was detected in the inflorescence meristem (Supplemental Fig. S3E).

Effect of Ectopic Expression of *OSHB* Genes on Shoot Development

To gain further understanding of the rice Class III HD-Zip genes, we constructed ectopic-expressers of *OSHB1*, *OSHB3*, and *OSHB5*. Regenerated plants containing these cDNAs driven by the *ACTIN* promoter did not show morphological abnormalities, probably due to *miR166*-mediated posttranscriptional gene silencing. Therefore, we constructed *miR166*-resistant versions of the *OSHB1*, *OSHB3*, and *OSHB5* cDNAs driven by the *ACTIN* promoter, each of which contained five mutations at the *miR166*-binding site that did not cause amino acid substitutions (Supplemental Fig. S1B), and transformed them into wild-type calli. We

obtained 12, 14, and nine independent transgenic plants harboring the mutated *OSHB1* (*OSHB1m*), *OSHB3m*, and *OSHB5m*, respectively.

Transgenic plants containing *OSHB3m* showed the most severe phenotype, those containing *OSHB1m* showed a less severe phenotype, and those containing *OSHB5m* showed a weak phenotype (Fig. 5A). Two types of abnormal leaves were observed: rolled leaves and filamentous leaves (Table I). The rolled-leaf phenotype was further categorized into three types based on severity. Type I plants had adaxially rolled leaves with a normal leaf blade-sheath boundary (Fig. 5, B and F). All *OSHB5m* plants were categorized into this type (Table I). The intermediate phenotype, Type II, had adaxially rolled leaves with ectopic ligules. In wild-type leaves, the ligule is formed on the adaxial surface of the leaf blade-sheath boundary (Fig. 5B). In the Type II leaves, ligules formed on both the adaxial and abaxial surfaces of the leaf blade-sheath boundary (Fig. 5C). In addition, the leaf sheath of this type was twisted and whitish. Most of the *OSHB1m* plants showed Type II leaves (Table I). Type III plants exhibited narrow rolled leaves with ectopic ligules on the abaxial side of the blade-sheath boundary, and leaf sheath of the leaves was rough and had a complex shape (Fig. 5D). Type III plants were observed at a low frequency in *OSHB1m* plants and frequently in *OSHB3m* plants (Table I). Filamentous leaves, the most severe phenotype, were observed in half of the *OSHB3m* plants (Table I; Fig. 5A). Some filamentous leaves had a ring-like structure at the blade-sheath boundary (Fig. 5E), although most of these leaves did not have a ligule- and auricle-like structure and their blade-sheath boundaries were not obvious.

Next, we performed anatomical and morphological analyses on the transgenic plants. Blades of Type II *OSHB1m* leaves showed a reduction in abaxial sclerenchymatous cells and the ectopic formation of bulliform-like cells on the abaxial surface (Fig. 6, A and E). In the leaf sheath, most abaxial mesophyll cells were lost (Fig. 6, B, C, F, and G), which was a possible cause of the whitish appearance of the leaf sheath. Papillae were not observed on the abaxial epidermis of the *OSHB1m* leaf sheath, as in the adaxial epidermis of the wild-type sheath (Fig. 6, D and H). Despite these abnormalities, the vascular bundles appeared normal in the Type II leaves of *OSHB1m* plants. Thus, the ectopic expression of *OSHB1m* causes partially adax-

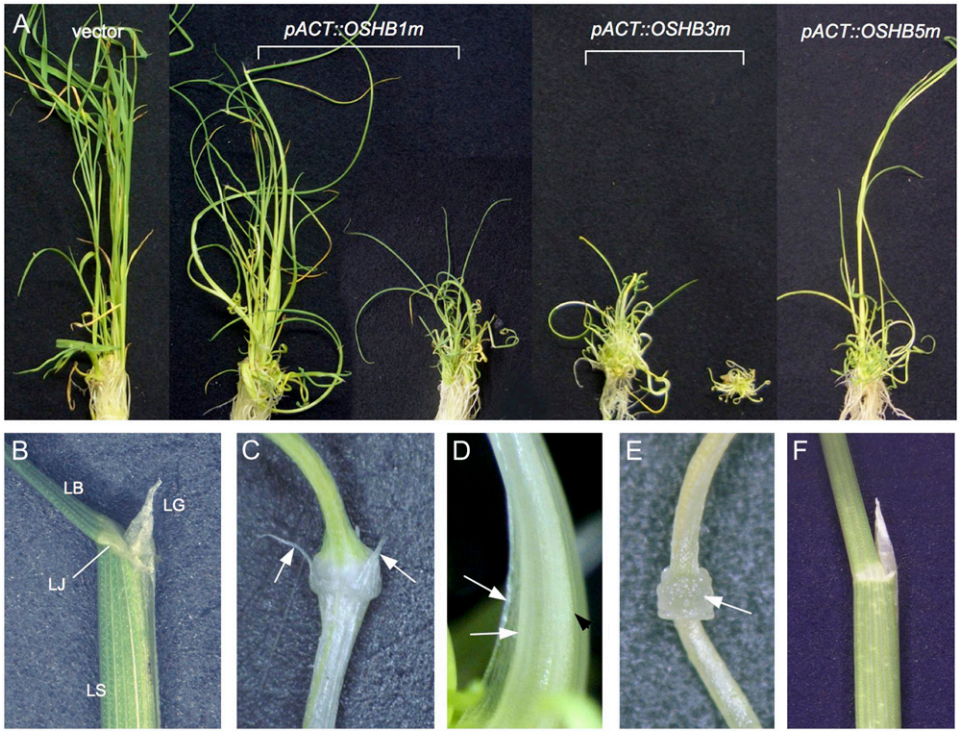

Figure 5. Phenotypes of transgenic plants expressing *miR166*-resistant *OSHB1, OSHB3,* and *OSHB5.* A, Control and transgenic plants at 1 month after regeneration. From left to right, control plant introduced with empty vector; *pACT*::*OSHB1m* plant showing mild phenotype; *pACT*::*OSHB1m* plant showing severe phenotype; *pACT*::*OSHB3m* plant showing mild phenotype; *pACT*::*OSHB3m* plant showing severe phenotype; and *pACT*::*OSHB5m* plant. B, Leaf blade-sheath boundary of the control leaf. LB, Leaf blade; LS, leaf sheath; LJ, lamina joint; LG, ligule. C, Blade-sheath boundary of the Type II *pACT*::*OSHB1m* leaf. Arrows show ligules formed on the abaxial sides. D, Complex-shaped leaf sheath of the Type III *pACT*::*OSHB3m* plant. Arrows indicate leaf margins and the arrowhead indicates an additional ridge on the abaxial side of the leaf. E, Blade-sheath boundary of the filamentous leaf in the *pACT*::*OSHB3m* plant. Arrow indicates the ring-like swell at the leaf blade-sheath boundary. F, Blade-sheath boundary of the Type I *pACT*::*OSHB5m* leaf. [See online article for color version of this figure.]

Table I. *Frequency of leaf phenotypes in OSHBm transgenic plants*

Transgene	Rolled Leaf[a]			Filamentous Leaf	n[b]
	Type I	Type II	Type III		
pACT::OSHB1m	0	10	2	0	12
pACT::OSHB3m	0	0	7	7	14
pACT::OSHB5m	9	0	0	0	9

[a]Rolled leaf phenotype was categorized into three types based on their severity: Type I, rolled leaf with no ectopic ligule; Type II, rolled leaf with ectopic ligules; Type III, rolled but complex-shaped leaf with ectopic ligules. [b]*n* indicates the total number of transgenic plants observed.

ialized leaves, but its effect is limited to the epidermis and subepidermal tissues.

Cross sections and scanning electron microscope (SEM) views of complex-shaped leaves in Type III *OSHB3m* plants revealed that the cause of the complexity was the formation of ectopic leaf margin-like structures from the leaves (Fig. 6, I, J, and M–O). Most of the ectopic structures resembled the membranous margin of wild-type leaves (Fig. 6, I and J). In an extreme case, leaf margin-like membranous structures formed directly from the base of the preexisting leaf primordia (Fig. 6, J and O). Because membranous structure of leaf margins in the wild type are established at the margins of SAM-derived leaf primordia, the ectopic margins are likely recruited independent of the main part of the leaf.

The filamentous leaves observed in *OSHB3m* plants were radialized (Fig. 6K). The vascular bundles were also radialized, with xylem surrounding phloem (Fig. 6L). The radialized leaves are likely produced ectopically from the stem, because no SAM-like structures were apparent at the axils of these filamentous leaves (Fig. 6P). Two *OSHB3m* plants formed spike-like leaves. Most were positioned randomly and appeared to be radialized (Fig. 6Q).

Type I leaves of *OSHB5m* plants did not show obvious abnormalities (Fig. 6R). However, abnormal vascular bundles were observed in some leaves (Fig. 6, S and T). The vascular bundles are sometimes radialized, and xylem tissues are poorly differentiated. This indicates that *OSHB5* has less of a function in leaf polarity, but is involved in vascular bundle patterning and differentiation. This is in contrast with *OSHB1m* plants, in which leaf abnormalities were observed mainly in the epidermis and subepidermal tissues but not in the vascular tissues.

To clarify how the introduction of *OSHBm* transgenes affects leaf polarity, we first examined the expression levels of the *OSHB* genes using real-time RT-PCR. In *OSHB5m* plants, the expression levels dramatically increased (Fig. 7A). However, in *OSHB1m* and *OSHB3m* plants, a relatively low level of increase in expression was observed. Next, we examined the expression of *OSHB3* in severe *OSHB1m* shoots, by in situ hybridization. *OSHB3* transcripts were ectopically detected in the adaxial and abaxial epidermis of P2 to P3 leaf primordia (Fig. 7B). Considering that the *OSHB3* transcript did not increase quantitatively in *OSHB1m* shoots (Fig. 7A), leaf adaxialization in *OSHB1m* is a direct cause of the ectopic expression and/or overexpression of *OSHB1m*, and the ectopic *OSHB3* expression in *OSHB1m* leaves is a secondary effect of the leaf adaxialization. Reciprocally, *OSHB1* transcripts in *OSHB3m* shoots were distributed in both the adaxial and abaxial epidermis of P2 to P3 leaf primordia, indicating that the ectopic expression and/or overexpression of *OSHB3m* caused leaf adaxialization (Fig. 7C). However, the adaxialization did not occur in all leaf tissues, and the adaxial/abaxial polarity was maintained in the leaf margins. No ectopic expression of *OSHB3* was detected on the abaxial sides of the *OSHB5m* leaves. However, the level of *OSHB3* expression in the xylem tissue of the several vascular bundles was lowered (Fig. 7D). Thus, the introduction of the *OSHB1m* and *OSHB3m* transgenes driven by the *ACTIN* promoter affects the adaxial-abaxial patterning of leaves. However, ectopically expressed *OSHB5m* does not affect leaf polarity, but influences vascular development.

Effect of Auxin Treatment on *OSHB* Expression

The expression of one of the Arabidopsis Class III HD-Zip genes, *ATHB8*, is induced by auxin (Baima et al., 1995), and a possible interaction between auxin and/or auxin flow and Class III HD-Zip genes in Arabidopsis has been proposed (Bowman and Floyd, 2008). To examine the effect of auxin on the expression of the *OSHB* genes, we first treated rice seedlings with 1 μM 2,4-dichlorophenoxyacetic acid (2,4-D) for 3 to 24 h, and examined the expression levels of the five *OSHB* genes using real-time RT-PCR. The expression of the *OSHB1* and *OSHB3* genes was not significantly affected by 2,4-D treatment, whereas the expression of *OSHB2*, *OSHB4*, and *OSHB5* had increased at 12 and 24 h after 2,4-D treatment. In contrast, the expression of *OsIAA9*, one of the early auxin response AUX/IAA-family genes (Jain et al., 2006), increased dramatically at 3 and 6 h after 2,4-D treatment (Fig. 8A).

We next investigated the long-term effect of auxin treatment on rice seedling development and *OSHB* expression. Seedlings grown for 2 weeks in culture medium containing 1 μM 2,4-D showed reduced leaf length, the formation of thick and tube-like leaves, and the inhibition of leaf initiation and root elongation (Fig. 8B). In these plants, the expression of *OSHB3* in the SAM was dramatically enhanced (Fig. 8, C and D; compare with Fig. 3, C and H). Unlike the localized expression of *OSHB3* in the central domain of the untreated SAM, the expression was extended to the whole region of the 2,4-D-treated SAM (Fig. 8, E and F). Concurrently, the SAM was vertically elongated. However, *OSHB3* expression in the adaxial domain and the vascular bundles of young leaf primordia was not affected (Fig. 8, C and D). In addition, polarity defects were not observed in either the leaf primordia

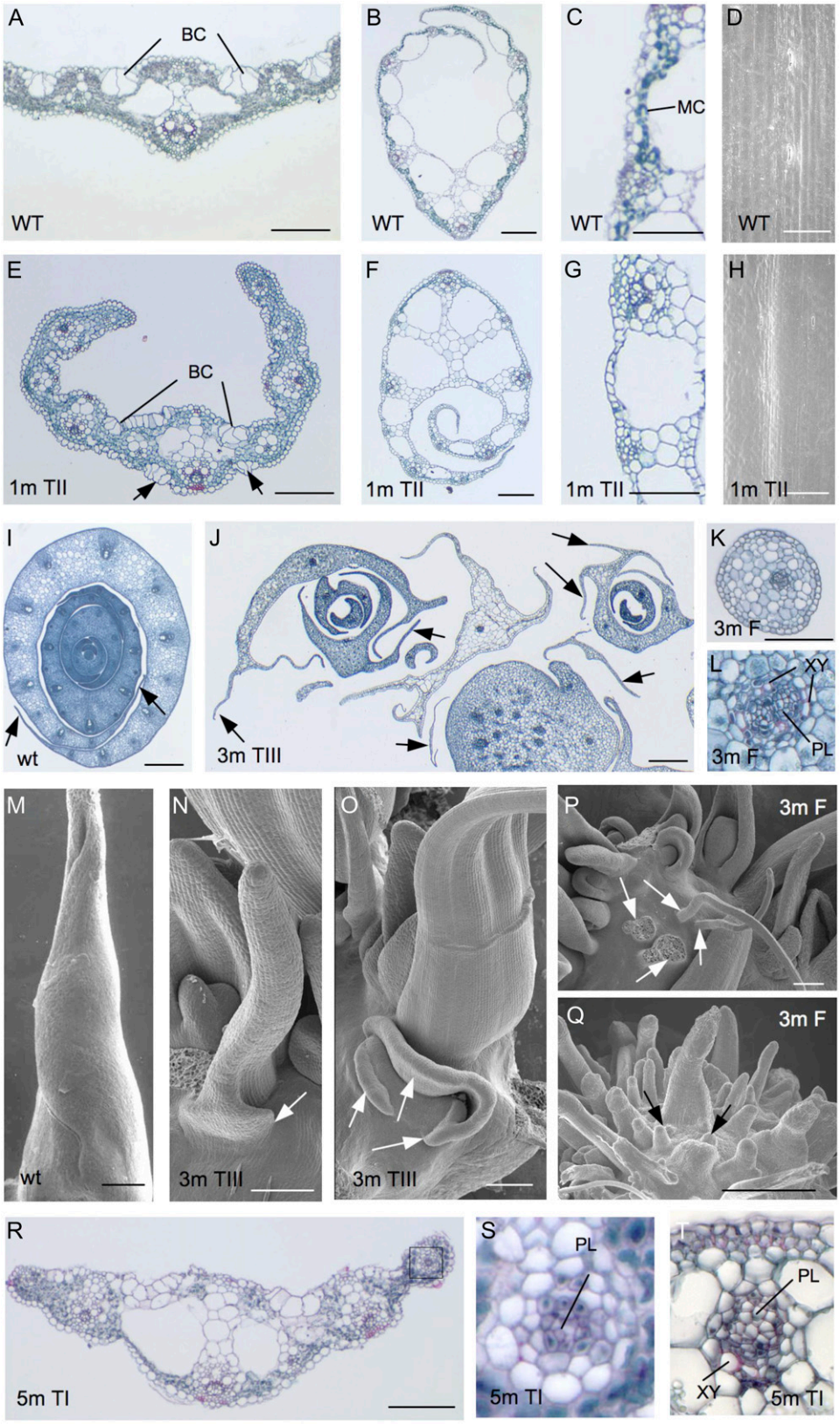

Figure 6. Leaf and shoot apex morphology of *pACT*::*OSHBm* transgenic plants. A, Cross section of the wild-type leaf blade. Bulliform cells (BC) are observed at the adaxial surface. B, Cross section of the wild-type leaf sheath. C, Close-up view of the abaxial side of the wild-type leaf sheath with dark-stained mesophyll cells (MC). D, Adaxial surface view of the wild-type leaf sheath lacking papillae. E, Cross section of the *pACT*::*OSHB1m* leaf blade, showing ectopic formation of bulliform cells (BC) on

or the vascular bundles, although the shape of the leaf primordia was abnormal and the vascular bundles were unequally distributed along the lateral direction of the leaf (Fig. 8D). A similar expression pattern was observed when the *OSHB1* and *OSHB4* genes were used as a probe (data not shown).

To better understand how leaf primordia initiate in the 2,4-D-treated SAM, we examined the expression pattern of the Class I *KNOX* gene *OSH1*, whose down-regulation is a marker of P0 leaf primordium (Sentoku et al., 1999). Down-regulation of *OSH1* was observed in a small group of cells (P0 primordium) in the normal SAM (Fig. 8G). However, in 2,4-D-treated plants, *OSH1* down-regulation occurred in the vertically extended domain of the flank of the SAM (Fig. 8H). This expression pattern indicates that leaf founder cells required for the leaf primordium are distributed in a large cylinder-like domain of the entire SAM. This cylinder-like distribution of leaf founder cells is consistent with the thick and tube-like leaf primordia produced by 2,4-D treatment (Fig. 8, C and D).

To demonstrate that the aberrant leaf initiation was caused by ectopic *OSHB3* expression and not the result of geometrical alternation of the SAM or the long-term effect of auxin treatment, we observed *OSHB3* expression soon after the onset of auxin treatment. Ectopic expression of *OSHB3* in the SAM was observed as early as 6 h after 2,4-D treatment, when morphological changes in the SAM were not yet observed; the expression was maintained at least 24 h after the treatment (Fig. 8, I and J). This result indicates that ectopic *OSHB3* expression is quickly induced by auxin in the SAM, which may affect the normal leaf initiation processes.

DISCUSSION

Functional Conservation, Redundancy, and Differences among Rice Class III HD-Zip Genes

Five Class III HD-Zip genes of rice encode possible transcriptional regulators with well-conserved motifs that are present in all plant Class III HD-Zip genes. *OSHB1* to *OSHB4* are similar in both gene structure and expression patterns, suggesting their functional redundancy. In fact, a loss-of-function mutant of *OSHB4* having a *Tos17* insertion (Miyao et al., 2003) showed no obvious phenotype (data not shown). However, a detailed examination of the expression profiles of these genes revealed that they differ from one another. Phylogenetic analysis showed that *OSHB5* is distantly related to other *OSHB* genes. This finding is supported by an analysis of the gene structure and the expression profile.

Transgenic analysis also revealed diverse functions for the *OSHB* genes. Adaxially rolled leaves were commonly observed in the *OSHB1m*, *OSHB3m*, and *OSHB5m* plants, but *OSHB5m* did not exhibit leaf polarity defects. Ectopic ligules were observed in both the *OSHB1m* and *OSHB3m* plants, but radialized leaves were observed only in the *OSHB3m* plants. Thus, *OSHB3* may contribute more to leaf polarity than *OSHB1*. The radially symmetric vascular bundles of the *OSHB3m* and *OSHB5m* plants indicate that *OSHB3* and *OSHB5* are involved in vascular patterning and differentiation. In contrast, the *OSHB1m* plants exhibited no vascular defects. The expression level of *OSHB1* in *OSHB1m* transgenic plants and *OSHB3* in *OSHB3m* was not dramatically elevated; one possible explanation for this is that strong *OSHB1m* and *OSHB3m* expression may be lethal to regenerating plants.

The conservation of *miR166*-binding sequences among the five *OSHB* genes indicated that all of the genes are potentially regulated by *miR166*. Indeed, transgenic plants containing the *OSHB1*, *OSHB3*, or *OSHB5* genes driven by the *ACTIN* promoter showed no obvious phenotypes, whereas when *OSHB1*, *OSHB3*, and *OSHB5* with mutations in the *miR166*-binding site were introduced, the resulting transgenic plants exhibited abnormal phenotypes. Thus, *miR166*-mediated gene silencing contributes to the regulation of *OSHB* expression. However, our transgenic analysis using a constitutive *ACTIN* promoter, makes it difficult to know how *OSHB* genes are spatially and quantitatively regulated by *miR166*. In fact, phenotypes of gain-of-function allele of the maize *RLD1* gene, which

Figure 6. (*Continued.*)
the abaxial side. F, Cross section of the *pACT*::*OSHB1m* leaf sheath. G, Close-up view of the abaxial side of the *pACT*::*OSHB1m* leaf sheath. H, Abaxial surface view of the *pACT*::*OSHB1m* leaf sheath lacking papilla. I, Cross section of the wild-type shoot apex. Arrows show membranous leaf margins. J, Cross section of the *pACT*::*OSHB3m* shoot apex. Arrows show ectopic leaf margins. K, Cross section of the *pACT*::*OSHB3m* filamentous leaf. L, Close-up view of the vascular bundle of the *pACT*::*OSHB3m* filamentous leaf. Phloem (PL) is surrounded by xylem (XY) tissue. M, SEM image of wild-type leaf primordium. N, SEM image of the *pACT*::*OSHB3m* shoot apex, in which the ectopic leaf margin (arrow) is formed. O, SEM image of the *pACT*::*OSHB3m* shoot apex showing ectopic formation of leaf margin-like structures (arrows) that are formed independently from the abaxial base of the leaf. P, SEM image of the *pACT*::*OSHB3m* plant showing multiple shoots and filamentous leaves (arrows) without shoot meristem at their axils. Q, SEM image of the *pACT*::*OSHB3m* plant with enormous spike-like leaves. Leaf primordia-like structures (arrows) are observed between the preexisting leaves. R, Cross section of the *pACT*::*OSHB5m* leaf blade. S, Close-up view of the vascular bundle of the *pACT*::*OSHB5m* leaf in R with phloem (PL) surrounded by bundle sheath cells and underdeveloped xylem tissue. T, Close-up view of the vascular bundle of the *pACT*::*OSHB5m* leaf with fully differentiated phloem (PL) and reduced xylem (XY) tissue. Scale bar = 100 μm in A, B, E, F, J, M to R; 50 μm in C, D, G, H, and K; 500 μm in I. Phenotypic categories and genotypes are labeled in the images; WT, Wild type; 1 m, *OSHB1m*; 3 m, *OSHB3m*, 5 m, *OSHB5m*; TI, Type I; TII, Type II; TIII, Type III; F, filamentous leaf (see Table I). [See online article for color version of this figure.]

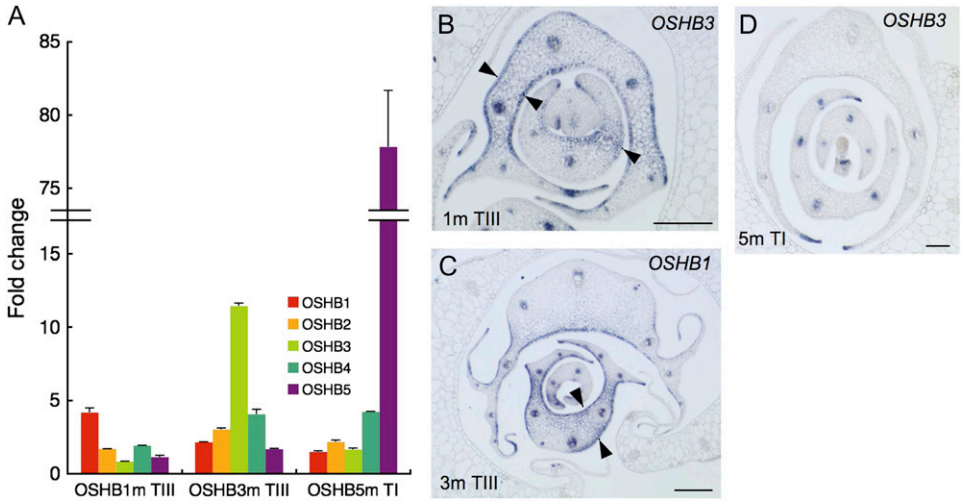

Figure 7. Effect of *pACT::OSHBm* expression on leaf polarity. A, Real-time RT-PCR analysis of five *OSHB* genes in *pACT::OSHB1m* plants showing Type III phenotype (see Table I; left), in Type III of *pACT::OSHB3m* (middle), and in Type I of *pACT::OSH5m* (right). Fold-change relative to the vector control plant is shown. Expression level was normalized to that of *eEF-1α*. Bars indicate SD. B, In situ localization of *OSHB3* transcripts in Type III *pACT::OSHB1m* shoot apex. Arrowheads indicate *OSHB3* expression on both the adaxial and abaxial sides of the leaf primordia. C, In situ localization of *OSHB1* transcripts in Type III *pACT::OSHB3m* shoot apex. Arrowheads indicate *OSHB1* expression on both the adaxial and abaxial sides of the leaf primordia. D, In situ localization of *OSHB3* transcripts in Type I *pACT::OSHB5m* shoot apex. Scale bars in B to D =100 μm.

is an ortholog of *OSHB1*, are considerably weaker than those of *OSHB1m* (Juarez et al., 2004). Thus, analyses of similar transgenic experiments using *OSHB* endogenous promoters and of their gain-of-function mutants are needed for further understanding of the *miR166*-mediated regulation.

Role of *OSHB* Genes in Embryogenesis

The *OSHB3* gene was first expressed in a small group of cells in the center of the early globular embryo, and additional expression of *OSHB1*, *OSHB3*, and *OSHB4* appeared in the ventral domain of the embryo, where the SAM and coleoptile primordium will initiate. This expression pattern in the early embryo is different from that of the Arabidopsis orthologs of the gene. In Arabidopsis, the *REV*, *PHB*, and *PHV* genes are expressed at the apical and central poles of early globular embryos, which is important for the radial patterning of the apical region and SAM formation (McConnell et al., 2001; Emery et al., 2003; Prigge et al., 2005). The early expression in the embryo indicates that the *OSHB* genes may also participate in radial pattern formation in the rice embryo. If so, the central expression of *OSHB* is involved in radial patterning in the early globular embryo, and subsequent additional ventral expression is necessary to establish the SAM or shoot axis. This expression pattern suggests that Class III HD-Zip proteins function in radial patterning and SAM establishment could be separable. This is consistent with the analysis of *shootless* mutants of rice, which lack the ventral expression of the *OSHB* genes in the globular embryo (Nagasaki et al., 2007). In the *shootless* mutants, despite the complete loss of the embryonic shoot, embryo polarity and the other embryonic organs are normal (Satoh et al., 1999; Nagasaki et al., 2007). Accordingly, one of the functions of *OSHB* in embryogenesis is SAM establishment in the ventral domain of the embryo.

The involvement of *OSHB* in SAM initiation is also suggested by the *OSHB3m* transgenic plants, in which multiple shoots are produced not only at the axils of leaves but also at irregular positions. This means that the overexpression or ectopic expression of *OSHB3m* can induce the de novo formation of the SAM. In accordance with this, overexpressed *OSHB1m* can induce the formation of adventitious shoots from the callus of rice *shoot organization* mutants, which are defective in shoot regeneration (Nagasaki et al., 2007). Thus, *OSHB* genes should be associated with SAM formation not only in embryogenesis but also in the regeneration process.

Role of the *OSHB* Genes in Leaf Development

In Arabidopsis, three of the five Class III HD-Zip genes (*REV*, *PHB*, and *PHV*) regulate leaf polarity (Prigge et al., 2005). *OSHB1* to *OSHB4* are also involved in leaf polarity, as evidenced by the adaxialized leaves of the *OSHB1m* and *OSHB3m* plants. Radially symmetric leaves in severe *OSHB3m* plants did not seem to differentiate from the SAM. The spatial arrangement of filamentous leaves did not follow any obvious phyllotaxis, and no SAM-like structures were ever observed at the axils of filamentous leaves. Accordingly, *OSHB3* has the ability to induce leaf initiation independent of the SAM. A similar situation has been observed in triple mutants in *KAN* genes in

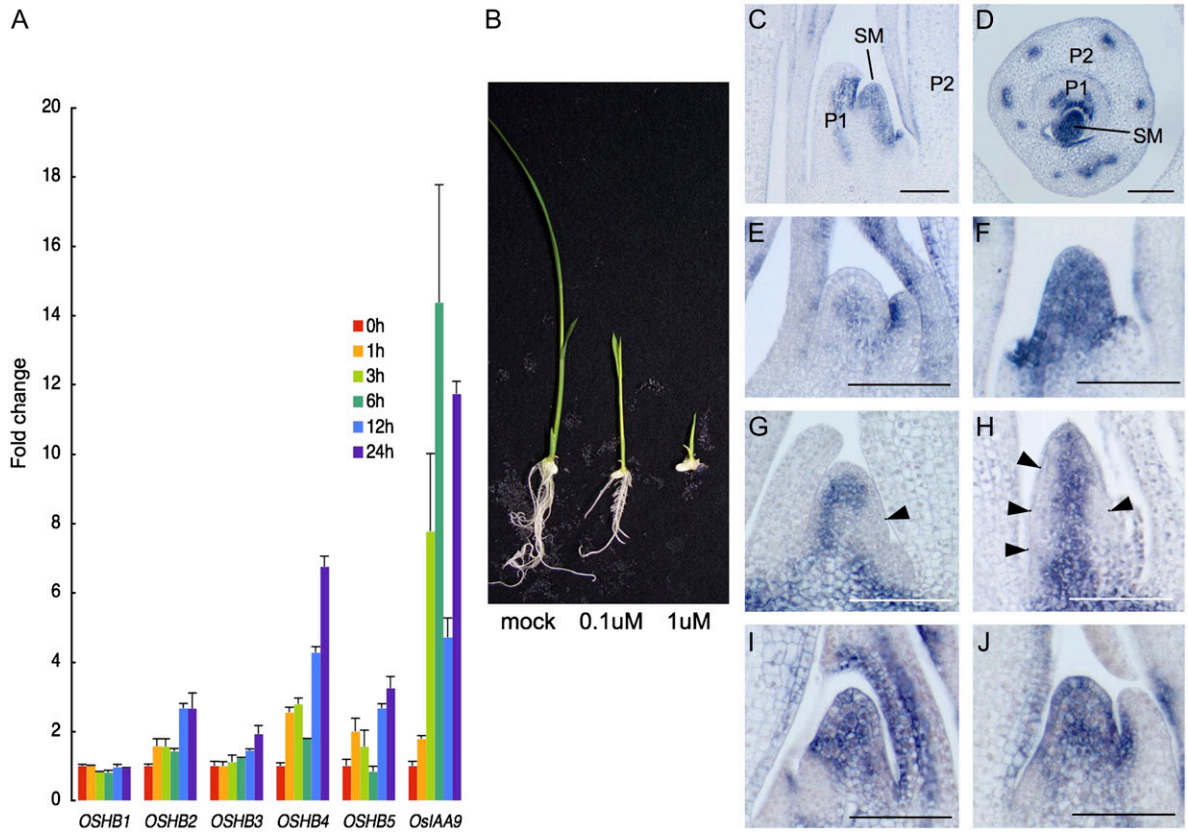

Figure 8. Effect of auxin treatment on *OSHB* gene expression. A, Real-time RT-PCR analysis of five *OSHB* genes and *OsIAA9*. Fold-change relative to the control plant at 0 h after 2,4-D treatment for each gene is shown. Expression level was normalized to that of *eEF-1α*. Bars indicate SD. B, Phenotypes of 2,4-D-treated plants 1 week after germination grown in culture media containing 0 μM (left), 0.1 μM (middle), and 1 μM (left) 2,4-D. C and D, *OSHB3* expression in longitudinal and cross sections of the shoot apex at 1 week after 2,4-D treatment. SM, SAM; P1, P1 leaf primordium; P2, P2 leaf primordium. E, *OSHB3* expression in the shoot apex without 2,4-D treatment. F, *OSHB3* expression in the SAM at 1 week after 2,4-D treatment. G, *OSH1* expression in the shoot apex without 2,4-D-treatment. Arrow shows down-regulation of *OSH1* on one side of the flank of the SAM. H, *OSH1* expression in the SAM at 1 week after 2,4-D treatment. Arrows indicate down-regulation of *OSH1* (arrow) along the peripheral domain of the SAM. I, *OSHB3* expression in the SAM at 6 h after 2,4-D treatment. J, *OSHB3* expression in the SAM at 24 h after 2,4-D treatment. Scale bars in C to J =100 μm.

Arabidopsis (Izhaki and Bowman, 2007); *kan1 kan2 kan4* embryos allow ectopic auxin maxima on the hypocotyls, resulting in leaf-like outgrowths without the expression of meristem markers. In Arabidopsis, activity of Class III HD-Zip genes and *KAN* genes is complementary and antagonistic (Eshed et al., 2001, 2004; Kerstetter et al., 2001; Emery et al., 2003). Although the relationship between the rice *KAN* orthologs and *OSHB* genes is unknown, *KAN* orthologs of maize are also expressed in domains complementary to those of the Class III HD-Zip genes (Henderson et al., 2006). Thus, it is possible that the genetic pathway is conserved between Arabidopsis and rice, and the ectopic expression of *OSHBm* affects the expression of the *KAN* orthologs, allowing the initiation of radialized and ectopic leaves.

The expression of all rice Class III HD-Zip genes in vascular tissues suggests a possibility that these genes have some role in vascular development. The expression of *OSHB3* in xylem tissue and radialized and the formation of amphivasal vascular bundles in *OSHB3m* leaves suggest that *OSHB3* has a function in vascular polarity and patterning. In contrast to the other *OSHB* genes, *OSHB5* expression was observed in phloem tissues. However, *OSHB5m* plants did not show defects in phloem tissue, but rather showed aberrant xylem tissue differentiation and vascular polarity. *OSHB5* may be necessary for the proper patterning of vascular bundles through its expression in phloem tissue. Although Arabidopsis and *Zinnia* genes belonging to the same clade as *OSHB5* are expressed in the xylem and procambium tissue and promote xylem differentiation (Baima et al., 2001; Ohashi-Ito and Fukuda, 2003; Ohashi-Ito et al., 2005), *CNA* and *ATHB8* have functions antagonistic to *REV* in Arabidopsis in some cases (Prigge et al., 2005), and one of the lycophytes Class III HD-Zip genes, *SkC3HDZ1* of *Selaginella kraussiana*, is expressed in tissues complementary to those of *SkC3HDZ2* (Floyd and Bowman, 2006; Floyd et al., 2006). Thus, Class III HD-Zip genes

could have achieved intraspecific divergence of their functions, and the expression of *OSHB5* may reflect antagonistic roles to the rest of the Class III HD-Zip genes in vascular patterning, although the evolutionary meaning is unclear.

Induction of *OSHB* Expression by Auxin and Its Effect on the Leaf Initiation Process

The expression of the Arabidopsis Class III HD-Zip genes *PHB* and *REV* is localized in the center of the SAM and in the peripheral region where leaf initiation will occur (McConnell et al., 2001). However, the regulatory mechanism of the expression pattern is unknown. Our analysis revealed that *OSHB* expression is up-regulated rapidly in the SAM flank at the early stage of leaf initiation, and then disappears again from the flank in the middle P1 stage. This dynamic change of expression is reminiscent of the leaf determination process regulated by local auxin accumulation in the SAM. The leaf initiation site in the SAM is determined by the local auxin maximum established by polar auxin transport through the L1 layer (Reinhardt et al., 2003). Recent studies on the PIN1 protein in the SAM have also shown a possible relationship between the auxin concentration and *REV* expression (Heisler et al., 2005; Bowman and Floyd, 2008).

The induction of *OSHB3* expression by auxin in the SAM suggests that excess auxin disturbs the local auxin distribution in the SAM, resulting in the ectopic expression of *OSHB3*, which may specify all peripheral SAM cells as leaf founder cells. In addition, *OSHB3m* promotes leaf initiation. Therefore, we propose a simple model with regard to the relationship of auxin, Class III HD-Zip genes, and the leaf initiation process in the SAM. In the wild type, the local concentration of auxin established by polar auxin transport induces Class III HD-Zip gene expression, and then Class III HD-Zip genes promote the initiation of leaf founder cells. A role of Class III HD-Zip genes in organ initiation has been proposed by expression analysis in angiosperms and lycophytes (Prigge and Clark, 2006), and supported by the ectopic induction of radialized leaves in the *OSHB3m* plants. However, the promotion of leaf initiation by Class III HD-Zip genes may not be a direct regulation, but a result of the elimination of other genetic factors such as the *KAN* and Class I *KNOX* genes.

In situ experiments revealed that auxin treatment affected *OSHB* expression in the SAM and thus leaf initiation, but not in leaves. Altered auxin distribution affects the leaf initiation process, but has less effect on organ polarity (Reinhardt et al., 2000, 2003). The difference in the auxin sensitivity of the processes of leaf initiation and leaf development may be associated with the differential actions of Class III HD-Zip genes in the SAM and the leaf. Although it is not known how auxin induces *OSHB3* expression only in the SAM, one possibility is that the auxin responsiveness depends on posttranscriptional mRNA silencing of Class III HD-Zip genes by *miR166*. *miR166* accumulation has been observed in the abaxial domains of leaves, but not in the SAM of maize or rice (Juarez et al., 2004; Nagasaki et al., 2007). Consequently, the auxin responsiveness of Class III HD-Zip genes may be displayed in the SAM but masked in the leaf due to *miR166*-dependent mRNA degradation.

Conservation and Divergence of Class III HD-Zip Gene Functions in Rice and Arabidopsis

In Arabidopsis, Class III HD-Zip genes play roles in embryo patterning, SAM formation, organ polarity, and vascular development (Prigge et al., 2005). The present analysis revealed that *OSHB* genes are expressed in domains similar to those in which Arabidopsis Class III HD-Zip genes are expressed: in part of the SAM, in the adaxial cells of leaf primordia, and in vascular tissues. It is difficult to make a direct examination of the functional conservation between Arabidopsis and rice orthologs due to the lack of loss-of-function mutants in rice. However, the transgenic analysis may suggest that the functions of Class III HD-Zip genes are largely conserved between rice and Arabidopsis, because the order of phenotypic severity on leaf polarity between *OSHB3m*, *PHB/PHV* ortholog, and *OSHB1m*, *REV* ortholog, is in parallel with that between gain-of-function *PHB/PHV* and *REV* in Arabidopsis (Kerstetter et al., 2001; Zhong and Ye, 2004).

However, remarkable differences between the genes in these two organisms are also evident. *OSHB* genes are involved in leaf margin development, as evidenced by the *OSHB1* and *OSHB3* expression in leaf margins and the independent formation of leaf margin-like structures from the preexisting leaves in *OSHB3m* plants. In addition, *shoot organization* mutants of rice exhibit reduced levels of Class III HD-Zip expression and the loss of specific leaf domains, including leaf margins (Itoh et al., 2000). Unlike typical eudicots, the leaves of grasses and other monocots have a membranous leaf margin that is clonally distinct from the main part of the leaf (Scanlon and Freeling, 1997). Thus, Class III HD-Zip genes were probably utilized in the morphological innovation of the leaf during evolution, in which the membranous leaf margin characteristic of grasses and other monocots was established.

Alternatively, the functions of Class III HD-Zip genes associated with leaf margin development in rice may be related to stipule formation in some eudicots. In Arabidopsis, at least one Class III HD-Zip gene, *PHB*, seemed to be expressed in stipules (McConnell et al., 2001). In addition, ectopic stipules surrounding the entire leaf base have been observed in *phb-d* and *kan1 kan2*, both of which show excess amounts of Class III HD-Zip transcripts (Eshed et al., 2001, 2004). If ectopic stipule formation in Arabidopsis and ectopic leaf margin formation in rice are equivalent events, the leaf margin in grasses is homologous to the stipule in eudicots. This interpretation is consistent with the characteristics of the *narrow sheath* mutant in

maize (Nardmann et al., 2004). Although this issue must still be resolved, it is clear that Class III HD-Zip genes are involved in the diversification of leaves between rice and Arabidopsis.

CONCLUSION

Our results suggest that rice Class III HD-Zip genes are involved in key developmental processes that are conserved between rice and Arabidopsis, including embryo patterning, SAM initiation, leaf polarity, and vascular development. However, our findings indicate that rice Class III HD-Zip genes also regulate the leaf initiation process in an auxin-dependent manner. Furthermore, we have shown that Class III HD-Zip genes contribute to the morphological innovation and diversification of leaves in flowering plants.

MATERIALS AND METHODS

Plant Material

Rice plants (*Oryza sativa* 'Taichung 65') were used for this study. The plants were grown in a field or in a greenhouse at 30°C (day) and 25°C (night).

Isolation of the *OSHB5* Gene

Because only a partial cDNA corresponding to the *OSHB5* gene was found in the full-length cDNA database (KOME; http://cdna01.dna.affrc.go.jp/cDNA), a full-length *OSHB5* cDNA was amplified using one primer specific to the 3′ untranslated region of the partial *OSHB5* cDNA and another primer corresponding to a putative 5′ untranslated region sequence. The amplified fragment was inserted into pCR4 (Invitrogen) and sequenced.

Sequence and Phylogenetic Analysis

Full-length cDNAs of the *OSHB1* to *OSHB4* genes were identified in the rice full-length cDNA database, KOME. The splice sites of the *OSHB* genes were predicted by comparing the genomic sequences and their full-length cDNAs. The *miR166*-binding sequences of the five *OSHB* cDNAs were determined using the ClustalW program at the DNA Data Bank of Japan (http://www.ddbj.nig.ac.jp/). The Class III HD-Zip amino acid sequences of several species were identified by searching the public databases at the DNA Data Bank of Japan and the National Center for Biotechnology Information (http://www.ncbi.nlm.nih.gov/). Class III HD-Zip amino acid sequences were aligned using the ClustalW program at the DNA Data Bank of Japan, and then manually adjusted to optimize alignments using GENETYX software (Genetyx). The phylogenetic tree was constructed based on a full-length protein alignment generated with the neighbor-joining method using ClustalW and GENETYX, and then viewed and rooted using TREEVIEW (Page, 1996). The bootstrap values at the branching points were calculated from 1,000 replicates.

In Situ Hybridization

Samples were fixed in 4% paraformaldehyde in 0.1 M sodium phosphate buffer for 24 h at 48°C, and then dehydrated in a graded ethanol series. The dehydrated samples in 100% ethanol were replaced with xylene and embedded in Paraplast Plus (McCormick Scientific). Paraffin sections (8-μm thick) were applied to microscope slides coated with 3-aminopropyl triethoxysilane (Matsunami Glass). For the *OSH1* probe, the full-length cDNA was used as a template. The *OSHB1* and *OSHB2* probes were prepared as described elsewhere (Nagasaki et al., 2007). For the *OSHB3*, *OSHB4*, and *OSHB5* probes, a cDNA fragment was amplified by PCR and subcloned into pCR2.1 (Invitrogen) using primers specific to each gene (Supplemental Table S1). The probe lengths for *OSHB1* to *OSHB5* are 949 bp, 571 bp, 740 bp, 895 bp, and 750 bp, respectively. Among the five probes, the *OSHB1* probe shows the highest similarity with *OSHB2* mRNA (84.1%). Because no perfect overlap of the expression domains were observed between *OSHB1* and *OSHB2*, a possibility of cross-hybridization among the genes is weak in our experimental condition. Digoxigenin-labeled antisense and sense riboprobes were generated by digestion with *Spe*I and transcription with T7 RNA polymerase and DIG-RNA labeling mix (Roche). In situ hybridization and immunological detection of the hybridization signals were performed as described by Kouchi and Hata (1993).

Generation of Transgenic Plants

The mutant constructs of *OSHB1*, *OSHB3*, and *OSHB5* were generated from plasmids containing each *OSHB* cDNA by introducing five mutations into the predicted *miR166*-binding site (Supplemental Fig. S1) using a PCR-based site-directed mutagenesis method (Hemsley et al., 1989). The mutated cDNA fragments were inserted into the binary vector pBIAct1nos downstream of the *Act1* promoter in the sense orientation between the *Xba*I and *Sma*I sites (Kamiya et al., 2003). Expression vectors and control vectors that lacked the cDNA fragments were introduced into calli of the cultivar Taichung 65 via *Agrobacterium*-mediated genetic transformation (Hiei et al., 1994). Transgenic plants that regenerated from calli were placed and grown in Murashige and Skoog medium aseptically for 1 month, and then observed and sampled.

Histological Analysis

For paraffin sectioning, samples were fixed in formaldehyde-acetic acid solution (formaldehyde:glacial acetic acid:ethanol [1:1:18]) for 24 h at 4°C, dehydrated in graded ethanol series, and embedded as described above. Microtome sections (8-μm thick) were stained with Delafield's hematoxylin, safranin, or Fast-Green FCF and then observed with a light microscope. Dehydrated samples in 100% ethanol were infiltrated with 3-methyl-butylacetate, critical-point dried, sputter-coated with platinum, and observed under an SEM (S-4000; Hitachi) at an accelerating voltage of 10 kV.

Real-Time RT-PCR

Total RNA was extracted using TRIzol reagent (Invitrogen) according to the manufacturer's instructions. One microgram of RNA after DNase-I digestion was used for first-strand cDNA synthesis, and an RT reaction was performed using the High Capacity RNA-to-cDNA Master Mix (Applied Biosystems). The cDNA products were brought to a final volume of 200 μL, and 1.5 μL of the cDNA solution was subjected to amplification by real-time PCR. For quantification of the genes, Taq-Man assay was performed, using the TaqMan Fast Universal PCR Master Mix and FAM-labeled TaqMan MGB probes for each gene (Applied Biosystems), by the StepOnePlus real-time PCR system (Applied Biosystems). The expression level of each sample was normalized to that of an internal control, *eEF-1α*. The primers and Taq-Man MGB probes used to specifically detect *OSHB1* to *OSHB5*, *OsIAA9*, and *eEF-1α* are listed in Supplemental Table S1.

Auxin Treatment

For short-term treatment, 7-d-old seedlings were placed in sterilized water containing 1 μM 2,4-D whose stock had been dissolved in ethanol. The seedlings were sampled at 0, 3, 6, 12, and 24 h after treatment. As a negative control, we used 7-d-old seedlings treated for 24 h with sterilized water containing the same amount of ethanol as the 2,4-D treatment. For long-term treatment, seeds were sterilized in 2% sodium hypochlorite and inoculated and grown aseptically for 7 d on Murashige and Skoog medium containing 3% Suc; 1% agar (pH 5.8); and 0, 0.1, or 1 μM 2,4-D in a plant box at 28°C.

The GenBank accession numbers for the sequences described in the text and in Figure 1 and Supplemental Figure S1 are *OSHB1*, AK102378; *OSHB2*, AK102603; *OSHB3*, AK102183; *OSHB4*, AK103284; *OSHB5*, AB374207; *RLD1*, AY501430; *RLD2*, ABB89930; *ZeHB-10*, AB084380; *ZeHB-11*, AB084381; *ZeHB-12*, AB084382; *ZeHB-13*, AB109562; *REV/IFL1*, AF188994; *PHV/ATHB-9*, AJ440967; *PHB/ATHB-14*, Y11122; *CNA/ATHB-15*, AJ439449; *ATHB-8*, Z50851; and *PpHB10*, AB032182. The RAP locus codes for *OSHB1* to *OSHB5* are *Os03g0109400*, *Os10g0480200*, *Os12g0612700*, *Os03g0640800*, and *Os01g0200300*, respectively. The TIGR locus codes are *LOC_Os03g01890*, *LOC_Os10g33960*, *LOC_Os12g41860*, *LOC_Os03g43930*, and *LOC_Os01g10320*, respectively.

Supplemental Data

The following materials are available in the online version of this article.

Supplemental Figure S1. Alignment of HD-ZIP III proteins, and nucleotide and amino acid sequences at the *miR166*-binding site of the *OSHB1* to *OSHB5* genes.

Supplemental Figure S2. Real-time RT-PCR analysis of *OSHB* genes in various tissues.

Supplemental Figure S3. In situ localization of *OSHB* transcripts in reproductive phase.

Supplemental Table S1. Primers and TaqMan probes used in this study.

Received March 4, 2008; accepted June 16, 2008; published June 20, 2008.

LITERATURE CITED

Agalou A, Purwantomo S, Overnäs E, Johannesson H, Zhu X, Estiati A, de Kam RJ, Engström P, Slamet-Loedin IH, Zhu Z, et al (2008) A genome-wide survey of HD-Zip genes in rice and analysis of drought-responsive family members. Plant Mol Biol **66:** 87–103

Baima S, Nobili F, Sessa G, Lucchetti S, Ruberti I, Morelli G (1995) The expression of the *Athb-8* homeobox gene is restricted to provascular cells in *Arabidopsis thaliana*. Development **121:** 4171–4182

Baima S, Possenti M, Matteucci A, Wisman E, Altamura MM, Ruberti I, Morelli G (2001) The Arabidopsis ATHB-8 HD-ZIP protein acts as a differentiation-promoting transcription factor of the vascular meristems. Plant Physiol **126:** 643–655

Bowman JL, Floyd SK (2008) Patterning and polarity in seed plant shoots. Annu Rev Plant Biol **59:** 67–88

Chandler JW, Cole M, Flier A, Grewe B, Werr W (2007) The AP2 transcription factors DORNRÖSCHEN and DORNRÖSCHEN-LIKE redundantly control *Arabidopsis* embryo patterning via interaction with PHAVOLUTA. Development **134:** 1653–1662

Emery JF, Floyd SK, Alvarez J, Eshed Y, Hawker NP, Izhaki A, Baum SF, Bowman JL (2003) Radial patterning of *Arabidopsis* shoots by class III HD-ZIP and KANADI genes. Curr Biol **13:** 1768–1774

Eshed Y, Baum SF, Perea JV, Bowman JL (2001) Establishment of polarity in lateral organs of plants. Curr Biol **11:** 1251–1260

Eshed Y, Izhaki A, Baum SF, Floyd SK, Bowman JL (2004) Asymmetric leaf development and blade expansion in *Arabidopsis* are mediated by KANADI and YABBY activities. Development **131:** 2997–3006

Floyd SK, Bowman JL (2004) Gene regulation: ancient microRNA target sequences in plants. Nature **428:** 485–486

Floyd SK, Bowman JL (2006) Distinct developmental mechanisms reflect the independent origins of leaves in vascular plants. Curr Biol **16:** 1911–1917

Floyd SK, Zalewski CS, Bowman JL (2006) Evolution of class III homeodomain-leucine zipper genes in streptophytes. Genetics **173:** 373–388

Heisler MG, Ohno C, Das P, Sieber P, Reddy GV, Long JA, Meyerowitz EM (2005) Patterns of auxin transport and gene expression during primordium development revealed by live imaging of the *Arabidopsis* inflorescence meristem. Curr Biol **15:** 1899–1911

Hemsley A, Arnheim N, Toney MD, Cortopassi G, Galas DJ (1989) A simple method for site-directed mutagenesis using the polymerase chain reaction. Nucleic Acids Res **17:** 6545–6551

Henderson DC, Zhang X, Brooks L III, and Scanlon MJ (2006) RAGGED SEEDLING2 is required for expression of KANADI2 and REVOLUTA homologues in the maize shoot apex. Genesis **44:** 372–382

Hiei Y, Ohta S, Komari T, Kumashiro T (1994) Efficient transformation of rice (*Oryza sativa* L.) mediated by *Agrobacterium* and sequence analysis of the boundaries of the T-DNA. Plant J **6:** 271–282

Itoh JI, Kitano H, Matsuoka M, Nagato Y (2000) *SHOOT ORGANIZATION* genes regulate shoot apical meristem organization and the pattern of leaf primordium initiation in rice. Plant Cell **12:** 2161–2174

Itoh JI, Nonomura K, Ikeda K, Yamaki S, Inukai Y, Yamagishi H, Kitano H, Nagato Y (2005) Rice plant development: from zygote to spikelet. Plant Cell Physiol **46:** 23–47

Izhaki A, Bowman JL (2007) KANADI and class III HD-Zip gene families regulate embryo patterning and modulate auxin flow during embryogenesis in *Arabidopsis*. Plant Cell **19:** 495–508

Jain M, Kaur N, Garg R, Thakur JK, Tyagi AK, Khurana JP (2006) Structure and expression analysis of early auxin-responsive *Aux/IAA* gene family in rice (*Oryza sativa*). Funct Integr Genomics **6:** 47–59

Juarez MT, Kui JS, Thomas J, Heller BA, Timmermans MCP (2004) microRNA-mediated repression of *rolled leaf1* specifies maize leaf polarity. Nature **428:** 84–88

Kamiya N, Nagasaki H, Morikami A, Sato Y, Matsuoka M (2003) Isolation and characterization of a rice *WUSCHEL*-type homeobox gene that is specifically expressed in the central cells of a quiescent center in the root apical meristem. Plant J **35:** 429–441

Kerstetter RA, Bollman K, Taylor RA, Bomblies K, Poethig RS (2001) *KANADI* regulates organ polarity in *Arabidopsis*. Nature **411:** 706–709

Kouchi H, Hata S (1993) Isolation and characterization of novel nodulin cDNAs representing genes expressed at early stages of soybean nodule development. Mol Gen Genet **238:** 106–119

McConnell JR, Barton MK (1998) Leaf polarity and meristem formation in *Arabidopsis*. Development **125:** 2935–2942

McConnell JR, Emery J, Eshed Y, Bao N, Bowman J, Barton MK (2001) Role of *PHABULOSA* and *PHAVOLUTA* in determining radial patterning in shoots. Nature **411:** 709–713

Miyao A, Tanaka K, Murata K, Sawaki H, Takeda S, Abe K, Shinozuka Y, Onosato K, Hirochika H (2003) Target site specificity of the *Tos17* retrotransposon shows a preference for insertion within genes and against insertion in retrotransposon-rich regions of the genome. Plant Cell **15:** 1771–1780

Mukherjee K, Bürglin TR (2006) MEKHLA, a novel domain with similarity to PAS domains, is fused to plant homeodomain-leucine zipper III proteins. Plant Physiol **140:** 1142–1150

Nagasaki H, Itoh J, Hayashi K, Hibara K, Satoh-Nagasawa N, Nosaka M, Mukouhata M, Ashikari M, Kitano H, Matsuoka M, et al (2007) The small interfering RNA production pathway is required for shoot meristem initiation in rice. Proc Natl Acad Sci USA **104:** 14867–14871

Nardmann J, Ji JB, Werr W, Scanlon MJ (2004) The maize duplicate genes *narrow sheath1* and *narrow sheath2* encode a conserved homeobox gene function in a lateral domain of shoot apical meristems. Development **131:** 2827–2839

Ochando I, Jover-Gil S, Ripoll JJ, Candela H, Vera A, Ponce MR, Martinez-Laborda A, Micol JL (2006) Mutations in the microRNA complementarity site of the *INCURVATA4* gene perturb meristem function and adaxialize lateral organs in Arabidopsis. Plant Physiol **141:** 607–619

Ohashi-Ito K, Fukuda H (2003) HD-Zip III homeobox genes that include a novel member, *ZeHB-13* (*Zinnia*)/*ATHB-15* (*Arabidopsis*), are involved in procambium and xylem cell differentiation. Plant Cell Physiol **44:** 1350–1358

Ohashi-Ito K, Kubo M, Demura T, Fukuda H (2005) Class III homeodomain leucine-zipper proteins regulate xylem cell differentiation. Plant Cell Physiol **46:** 1646–1656

Otsuga D, Deguzman B, Prigge M, Drews G, Clark S (2001) *REVOLUTA* regulates meristem initiation at lateral positions. Plant J **25:** 223–236

Page RD (1996) TreeView: an application to display phylogenetic trees on personal computers. Comput Appl Biosci **12:** 357–358

Ponting CP, Aravind L (1999) START: a lipid-binding domain in StAR, HD-ZIP and signalling proteins. Trends Biochem Sci **24:** 130–132

Prigge MJ, Clark SE (2006) Evolution of the class III HD-Zip gene family in land plants. Evol Dev **8:** 350–361

Prigge MJ, Otsuga D, Alonso JM, Ecker JR, Drews GN, Clark SE (2005) Class III homeodomain-leucine zipper gene family members have overlapping, antagonistic, and distinct roles in *Arabidopsis* development. Plant Cell **17:** 61–76

Reinhart BJ, Weinstein EG, Rhoades MW, Bartel B, Bartel DP (2002) MicroRNAs in plants. Genes Dev **16:** 1616–1626

Reinhardt D, Mandel T, Kuhlemeier C (2000) Auxin regulates the initiation and radial position of plant lateral organs. Plant Cell **12:** 507–518

Reinhardt D, Pesce ER, Stieger P, Mandel T, Baltensperger K, Bennett M, Traas J, Friml J, Kuhlemeier C (2003) Regulation of phyllotaxis by polar auxin transport. Nature **426:** 255–260

Rhoades MW, Reinhart BJ, Lim LP, Burge CB, Bartel B, Bartel DP (2002) Prediction of plant microRNA targets. Cell **110:** 513–520

Satoh N, Hong SK, Nishimura A, Matsuoka M, Kitano H, Nagato Y (1999)

Initiation of shoot apical meristem in rice: characterization of four *SHOOTLESS* genes. Development **126:** 3629–3636

Scanlon MJ, Freeling M (1997) Clonal sectors reveal that a specific meristematic domain is not utilized in the maize mutant *narrow sheath*. Dev Biol **182:** 52–66

Sentoku N, Sato Y, Kurata N, Ito Y, Kitano H, Matsuoka M (1999) Regional expression of the rice *KN1*-type homeobox gene family during embryo, shoot, and flower development. Plant Cell **11:** 1651–1664

Sessa G, Steindler C, Morelli G, Ruberti I (1998) The Arabidopsis *Athb-8*, *-9* and *-14* genes are members of a small gene family coding for highly related HD-ZIP proteins. Plant Mol Biol **38:** 609–622

Steeves TA, Sussex IM (1989) Patterns in Plant Development, Ed 2. Cambridge University Press, Cambridge, UK

Talbert PB, Adler HT, Parks DW, Comai L (1995) The *REVOLUTA* gene is necessary for apical meristem development and for limiting cell divisions in the leaves and stems of *Arabidopsis thaliana*. Development **121:** 2723–2735

Tang G, Reinhart BJ, Bartel DP, Zamore PD (2003) A biochemical framework for RNA silencing in plants. Genes Dev **17:** 49–63

Zhong R, Taylor JJ, Ye ZH (1997) Disruption of interfascicular fiber differentiation in an *Arabidopsis* mutant. Plant Cell **9:** 2159–2170

Zhong R, Ye ZH (1999) *IFL1*, a gene regulating interfascicular fiber differentiation in *Arabidopsis*, encodes a homeodomain-leucine zipper protein. Plant Cell **11:** 2139–2152

Zhong R, Ye ZH (2001) Alteration of auxin polar transport in the Arabidopsis *ifl1* mutants. Plant Physiol **126:** 549–563

Zhong RQ, Ye ZH (2004) *amphivasal vascular bundle 1*, a gain-of-function mutation of the *IFL1/REV* gene, is associated with alterations in the polarity of leaves, stems and carpels. Plant Cell Physiol **45:** 369–385